by starting from the equilibrium configuration, but this can easily be tested in the following manner. We can follow Bloembergen's approach with a quantum treatment for the first few vibrational levels. We can then use the wave function of the molecule to get a starting probability distribution of initial configurations for a classical treatment of the later stages of the dissociation process. I have already mentioned the possible use of this kind of recipe for dealing with the zero point oscillations.

Another very great advantage of the suggested method is that the vague concepts of "leakage into the quasi-continuum" and diffusion into the continuum are avoided entirely. It is not necessary to introduce phenomenological rate and diffusion constants. It is also very easy to similate the effect of collisions in a classical treatment by subjecting one or more of the atoms of the molecule to random impulsive forces.

Calculations based on this program are now underway.

III. New Sub-Doppler Interaction Techniques

PROGRESS IN UNDERSTANDING SUB-DOPPLER LINE SHAPES

C.J. Bordé

Laboratoire de Physique des Lasers, Université Paris-Nord
Avenue J.-B. Clément, 93430 Villetaneuse, France

The application of sub-Doppler spectroscopic methods to optical frequency standards has stimulated many efforts to improve our knowledge of the line shapes in order to provide realistic estimates of the accuracy. In this paper we shall consider four directions of recent progress :

1- the recoil structure of the saturation resonances
2- transit effects on the line shapes and especially curvature-induced shifts
3- the influence of weak elastic collisions in saturation spectroscopy
4- the use of RAMSEY interference fringes in Doppler-free two-photon and saturation spectroscopies.

I - LIGHT SHIFT AND POLARIZATION DEPENDENCE OF THE RECOIL PEAKS

Owing to the atomic recoil during the interaction with light, every saturation resonance is usually a doublet (with the exception of crossover resonances). The origin of this doubling for a two-level system is illustrated in figure 1.

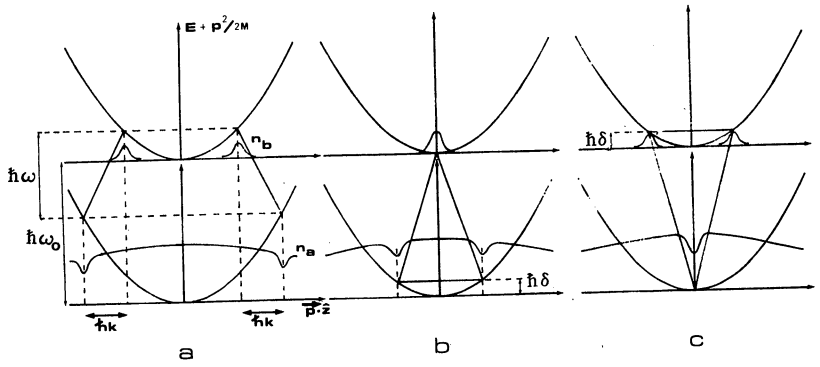

Figure 1

In a non-relativistic approximation, the curve representing the total energy versus the momentum component along the optical $\hat{z}$-axis is a parabola in each level. Because of momentum conservation, molecules interacting with a monochromatic field of a given direction have to belong to two different velocity classes in the lower and in the upper levels. The momentum change is precisely equal to the light quantum momentum $\pm\hbar k$ (where the sign depends upon the wave direction with respect to the $\hat{z}$-axis). There are two situations where one of the two waves can produce a change in the absorption of the other. The first (figure 1b) is obtained when molecules in the upper level can interact with both waves. The corresponding energy exchanged with the light can be read directly on the vertical axis. From the equation of the parabola it is easily seen that this energy is smaller than the Bohr energy $E_b - E_a$ by the amount $(\hbar k)^2/2M$. Similarly there is a second resonance obtained when molecules in the lower level can interact with both waves (figure 1c) and for which the energy exchanged is bigger than the Bohr energy by the same quantity. In first approximation each of these peaks has an intensity proportional to the lifetime of the velocity group in the corresponding level. This doublet structure was demonstrated with CH_4 at 3.39 µm, first in 1973 through a careful line shape study [1]. The 2.16 kHz splitting was then clearly resolved with large aperture parabolic optics to reduce the half-width below one kilohertz [2]. In fact Planck's constant measured by this method has a tendency to be too small and even to decrease with the light intensity ! This effect is now understood as a light shift of each recoil component towards the other, in a theory which treats one field to all orders and the probe field to first order [3]. In this approximation only four energy-momentum classes are coupled together by the light as illustrated on figure 2.

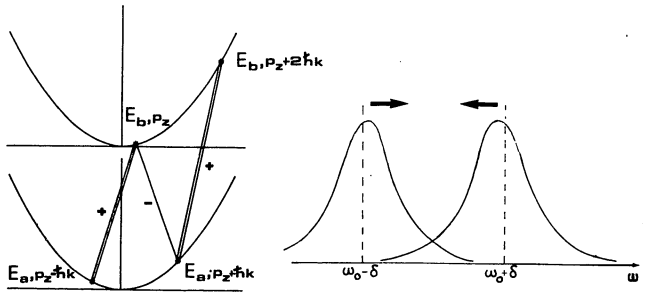

Figure 2

For plane waves this leads to a generalization of the BAKLANOV-CHEBOTAEV line shape :

$$\mathrm{Re}\sum_{\alpha=a,b}\Big[\gamma_{ba}+\Gamma-2i\,(\omega-\omega_o+\varepsilon_\alpha\delta)\Big]^{-1}\Big[\gamma_\alpha^{-1}-D_\alpha^{-1}\Big\{\Big(\gamma_{ba}+\Gamma-2i\,(\omega-\omega_o+\varepsilon_\alpha\delta)\Big)^{-1}$$

$$\Big[\Big(\gamma_{\beta\neq\alpha}+2\Gamma-2i\,(\omega-\omega_o+\varepsilon_\alpha\delta)\Big)^{-1}+\Big(\gamma_\alpha+2\Gamma-2i\,(\omega-\omega_o+3\varepsilon_\alpha\delta)\Big)^{-1}\Big]\,(\Omega^+)^2\gamma_\alpha^{-1}$$

$$+\tfrac{1}{2}\Big(\sqrt{1+S}-1\Big)\Big[\gamma_{\beta\neq\alpha}+2\Gamma-2i\,(\omega-\omega_o+\varepsilon_\alpha\delta)\Big]^{-1}\Big\}\Big]$$

with $\quad D_\alpha = 1+(\Omega^+)^2\Big[\Big(\gamma_\alpha+2\Gamma-2i\,(\omega-\omega_o+3\varepsilon_\alpha\delta)\Big)^{-1}+\Big(\gamma_{\beta\neq\alpha}+2\Gamma-2i\,(\omega-\omega_o+\varepsilon_\alpha\delta)\Big)^{-1}\Big]$

$$\Big[\Big(\gamma_{ba}+\Gamma-2i\,(\omega-\omega_o+\varepsilon_\alpha\delta)\Big)^{-1}+\Big(\gamma_{ba}+3\Gamma-2i\,(\omega-\omega_o+3\varepsilon_\alpha\delta)\Big)^{-1}\Big]$$

where $\quad \beta = a,b \;,\; \hbar\omega_o = E_b - E_a \;,\; \varepsilon_a = -1 \;,\; \varepsilon_b = +1 \;,$

$\gamma_\alpha, \gamma_{ba}$ are the relaxation constants for the population of level α and for the off-diagonal element of the density matrix,

$\Omega^+ = \mu_{ba}\,E_o^+/2\hbar$ is the Rabi pulsation for the matrix element μ_{ba} of the dipole operator and the amplitude E_o^+ of the saturating field

$S = 2\,(\Omega^+)^2\,(\gamma_a^{-1}+\gamma_b^{-1})/\gamma_{ba}$ is the saturation parameter,

and finally $\Gamma = \gamma_{ba}\sqrt{1+S}$, and $\delta = \hbar\omega_o^2/2Mc^2$

Besides the main contributions coming from population effects, we find contributions from higher order coherent processes, which are not symmetric with respect to the centers of each peak. These extra-contributions build up the inner side of each peak and thus lead to an apparent pulling of the peaks towards each other. In the limit of well resolved peaks the shift is given in first approximation by $(\Omega^+)^2/8\delta$ in circular frequency units. This light shift is a problem for optical frequency standards such as CH_4 at 3.39 µm and Ca at 6573 Å which are based on saturation lines for which the recoil doubling is not very large compared to the line-width. Other possible dependences of the line center with the light intensity come through the light shift caused by a third coupled level, differential saturation of any unresolved structure (recoil or hyperfine) [1] or differential saturation among transverse velocity classes changing the effective second-order Doppler shift [4]. Another interesting feature about the recoil doublet is the dependence of the relative intensities of the two components upon the polarization properties of the laser beams [5]. As an example let us consider the simple case of a $J = o \leftrightarrow J = 1$ transition such as the $^1S_0 \rightarrow {}^3P_1$ transition of

calcium at 6573 Å. With opposite circular polarizations of the counter-propagating beams (retro-reflected circularly polarized light) and the quantization axis chosen along the propagation axis, both beams induce σ^+ (or σ^-) transitions between M sublevels as illustrated on figure 3a.

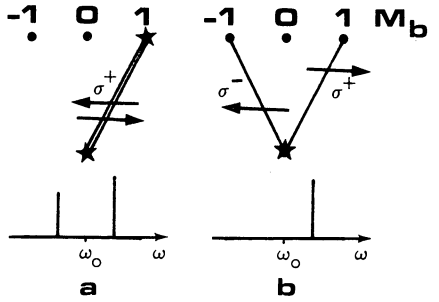

Figure 3

Both levels contribute symmetrically and, if the relaxation constants are approximately equal, the two recoil peaks have equal intensities. An identical conlusion is reached with parallel linear polarizations and is applicable to the CH_4 experiments. With identical circular polarizations, the two counter-propagating beams induce respectively σ^+ and σ^- transitions and only the crossover resonance of the J = o level is obtained. If the J = o level is the lower one, as on figure 3b, only the higher frequency recoil peak can occur. The same result is obtained for perpendicular linear polarizations. This property may be used to avoid the accuracy problem brought by the recoil structure. Closed-form formulae obtained by summing the corresponding products of Clebsch-Gordan coefficients are given in reference [5]. As another example, in the case of the F = 6 ↔ F = 7 transition of CH_4 at 3.39 µm and identical circular polarizations, the lower frequency recoil peak is 2.06 times bigger than the higher frequency one.

II - INFLUENCE OF TRANSIT EFFECTS ON THE LINE SHAPES - DENSITY MATRIX DIAGRAMS

In the high resolution limit the line shape is dominated by transit effects across the laser beam. It becomes essential to introduce in the equations the exact time-dependent perturbation corresponding to the shape of the pulse seen by the molecule in its flight across the beam. We have taken two approaches to this problem [4]. The first one is purely numerical : the coupled density matrix equations are solved with a computer and a numerical integration is performed on axial and transverse velocities. This method is especially useful for strong field problems (saturation effects) or arbitrary spatial dependence of the laser fields [6]. The second approach is a third order perturbation method which leads to analytical results [4].

During these studies density matrix diagrams have been a most useful tool [4,7]. It seems therefore appropriate to give first a brief introduction to these diagrams. The simplest process that one can consider is a single quantum transition of a molecule from level a to level b. The corresponding diagram is shown on figure 4a.

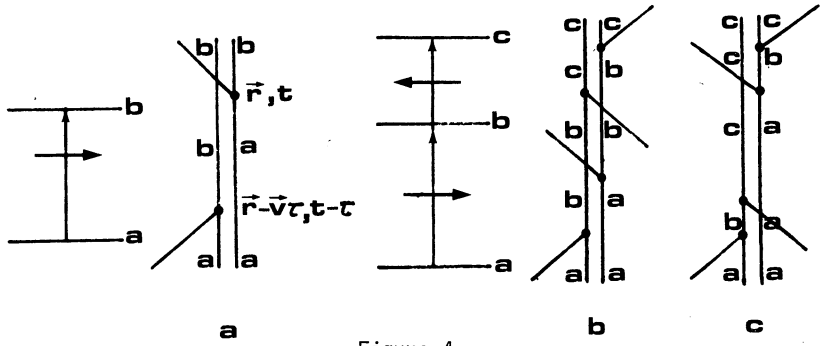

Figure 4

The density matrix elements for the molecule are represented by a vertical double bar along the time axis. To each segment corresponds a subscript of the matrix element $\rho_{aa'}$, $\rho_{ba'}$, $\rho_{bb'}$. Each interaction with the field is represented by a vertex between two segments. The field is represented by a lateral line coming from the right or from the left according to its direction with respect to the $\hat{z}$-axis. The field is separated in the exp (- iωt) part (line going upwards) and in the exp (iωt) part (line going downwards). At each vertex the rotating wave approximation leaves a single possibility between these two : on the first column the line has to go upwards when the subscript is changed from that of a lower energy level to a higher energy one (for example a to b on figure 4a) the line goes down when the corresponding energy decreases (b to a) and these rules are reversed on the second column. To each time interval τ appearing between two vertices and corresponding to the density matrix element $\rho_{\alpha\beta}$ we associate the propagator $\exp-(i\omega_{\alpha\beta} + \gamma_{\alpha\beta})\tau$. The diagram is terminated at space-time point $(\vec{r},t)$ by a last vertex. If the molecules have the velocity $\vec{v}$ the space-time coordinates of the previous vertices are determined by the various time intervals : $(\vec{r}-\vec{v}\tau,\ t-\tau)$, $(\vec{r}-\vec{v}\tau-\vec{v}\tau',\ t-\tau-\tau')$... The matrix element of the interaction hamiltonian for each vertex is taken at the corresponding space-time point : $V_{\alpha',\alpha}\ (\vec{r}-\vec{v}\tau-\vec{v}\tau'...,\ t-\tau-\tau'...)/i\hbar$ for a change from α to α' on the first column, $-V_{\beta\beta'}/i\hbar$ for a change from β to β' on the second column. Only the part of

the field corresponding to the line orientation is kept in the interaction hamiltonian. One has then to perform the integration over all time intervals $\tau,\tau'\ldots$ (from 0 to $+\infty$) of the products of all the quantities appearing on the diagram, times the initial equilibrium population. The diagram then gives the rate of change of the last density matrix element (usually a population) at space-time point $(\vec{r},t)$. To get a fluorescence signal or the absorbed power, final integrations over space and the velocity distribution need to be performed. The mathematical justification of these diagrams may be found in the Appendix A of reference [4] and a detailed example of application to Doppler-free two-photon spectroscopy is given in reference [7]. In the linear absorption diagram of figure 4a, the equilibrium population of the lower level ρ_{aa} is turned by a first interaction into the off-diagonal element ρ_{ba} which in turn will give rise to a change in the upper state population ρ_{bb} at the second vertex ; a second contribution comes from the complex conjugate diagram involving ρ_{ab}. For a plane wave the application of the preceding rules leads to the familiar VOIGT profile. As a second example, let us consider the three-level system of figure 4b interacting with two fields having opposite directions. If we put two of the previous diagrams in sequence, we get one of the diagrams representing stepwise excitation from level a to level b to level c. If we exchange the order of the two middle vertices, instead of going through the intermediate level population ρ_{bb}, the corresponding process goes through the off-diagonal element ρ_{ca} which has a resonant behaviour for the frequency ω_{ca} (figure 4c). The corresponding diagram is thus one of those describing Doppler-free two-photon spectroscopy [7]. If we finally turn to saturated absorption spectroscopy for a two-level system, the only two fourth-order diagrams of interest are represented on figure 5.

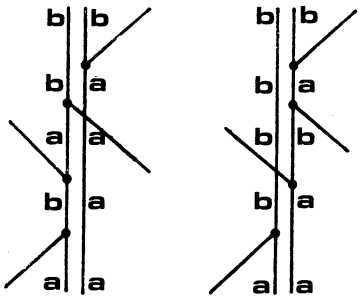

Figure 5

In a first process the lower state population is turned into an optical coherence which in turn gives a population hole in the lower state population. This hole is then probed by the opposite direction wave as described by the

two next interaction vertices. This diagram represents the higher frequency recoil peak and there is a similar diagram for the low frequency one, going through the upper state population change. For Gaussian laser beams, all the integrations but one may be performed analytically and the Fourier transform of the line shape for each recoil peak is obtained [4] :

$$\mathrm{Im}\int_0^{+\infty} d\tau\ \gamma_\alpha Y^{-1}\left[\exp(X-iY)E_1(X-iY)-\exp(X+iY)E_1(X+iY)\right]\ \exp\left\{2\left[i(\omega-\omega_o+\varepsilon_\alpha\delta)-\gamma_{ba}\right]\tau\right\}$$

where E_1 is the exponential integral function of the following arguments :
$X = \gamma_\alpha\ (B/A)\tau$, $Y = \gamma_\alpha\left(1 + Du^2\tau^2 - i\omega_o(u^2/c^2)\tau\right)^{1/2}/u\sqrt{A}$
A,B,D, are coefficients easily calculable from the beam geometry. The second order Doppler shift is included in Y. One may take advantage of having a Fourier transform to include the effect of the laser frequency modulation by multiplying the integrand by the proper Bessel function [4,8] or the broadening due to the laser frequency jitter with the help of the convolution theorem. This line shape formula describes fairly well the transit-time broadening and especially the line-width collapse at low pressures due to the anomalous contribution of slow molecules. The following interesting formula for the half-width was derived in [4] for this low pressure regime :
$\Delta\xi = \sqrt{\eta}\,2^{-\frac{1}{4}}\exp\left(\frac{3G}{\pi} - \frac{\Gamma}{2}\right)$ where the half-width and the relaxation constant are in units of the average reciprocal transit-time across the beam waist radius $\Delta\xi = \Delta\omega\ w_o/u$, $\eta = \gamma w_o/u$; G and Γ are respectively Catalan's and Euler's constants. The reduction in second-order Doppler shift in this regime is also well described by our line shape. Another new important result was brought by this theory : owing to the curvature of the wave-fronts, the coefficient B is usually complex and introduces a shift and an asymmetry in the line shape. A quick but rough physical explanation for this shift is the following : let us assume that we have a diverging saturation beam and a matched converging probe beam. The molecules entering on either side of this system first see a blue-shifted saturation beam because of the outwards component of its wave-vector. Part of this information (population hole or peak created) is carried across the beam by the molecular motion and probed at a later time by the probe beam which is also blue-looking for the molecules leaving the field region. The net result is a red shift of the resonance. This shift is exactly reversed if the roles of both beams are reversed. This effect is a very serious problem for the accuracy of optical frequency standards based on saturation spectroscopy since shifts of several hundred kilohertz have been observed. A quantitative demonstration of the effect has been performed with methane at 3.39 μm [8] and fortunately the agreement with

the calculated line shape is so good that one can feel confident enough in the present understanding of the physics to suggest conditions where this shift is very small and to calculate an upper limit of its value. The Fourier transform of the line shape has also been derived for Doppler-free two photon spectroscopy with Gaussian beams [7] :

$$\mathrm{Re}\int_0^{+\infty} d\tau\ (1+\beta u^2\tau^2 - i\omega_{ca}\tau u^2/2c^2)^{-1}\ (1-i\omega_{ca}\tau u^2/2c^2)^{-1/2}\ \exp\left\{\left[i(2\omega-\omega_{ca})-\gamma_{ca}\right]\tau\right\}$$

where β is a real parameter (that can be derived from the beam geometry) and thus no curvature-induced shift can occur in this case (for matched beams β is simply w^{-2}). The integration leads to simple formulae for the line shape when either the transit time broadening or the second-order Doppler shift may be neglected [7] .

III - INFLUENCE OF WEAK ELASTIC COLLISIONS ON THE LINE SHAPE

An important piece of physics is missing from our previous saturation line shape : there is a pressure range where weak elastic collisions may play

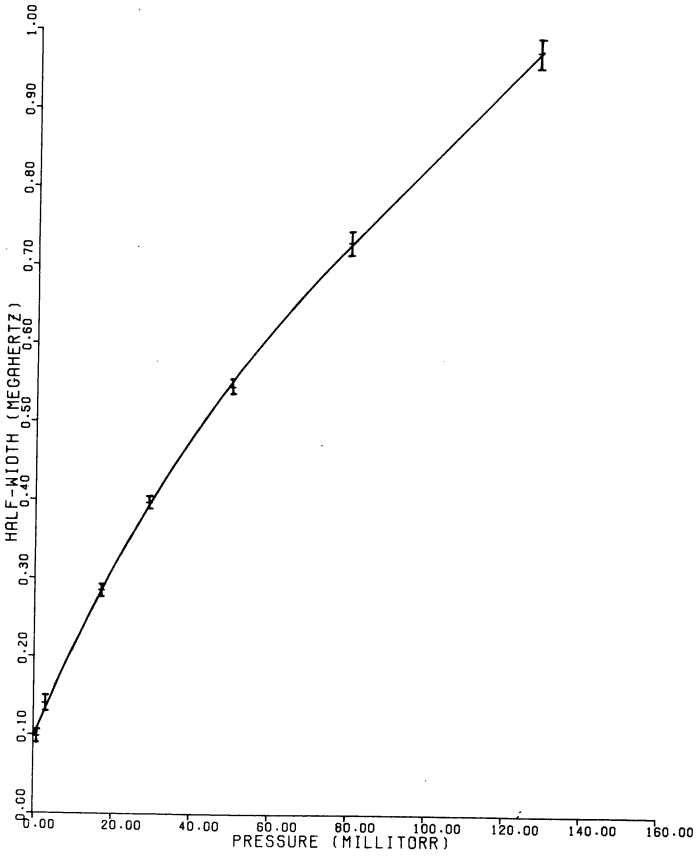

a major role in the broadening of saturation resonances. There has been an increasing set of experimental evidences for this, either from transient experiments [9] or directly from the anomalous behaviour of the broadening rate versus pressure [10,11] . As an example the figure 6 shows the width versus pressure of one of the iodine saturation peaks in coïncidence with the Argon laser at 5145 Å [11].

The non-linearity in this curve may be explained and even fitted by introducing weak elastic collisions in the theory. Other observations of this kind have been reported with molecules in the infrared : CH_4, CO_2, NH_3 [10]. We have been able to show, either by a fully diagrammatic approach or by taking the Fourier transform with respect to v_z [12], that the effect of these collisions may be simply introduced in the previous saturation line shape formulae by the following replacement rules :

$\gamma_\alpha \to \gamma_\alpha - \tilde{W}_\alpha(\tau)$, $\quad \gamma_{ba} \to \gamma_{ba} - \Phi(\tau)$ where $\tilde{W}_\alpha$ and Φ are obtained from the collision kernels W_α for the populations and W_{ba} for the off-diagonal density matrix element [12] by :

$$\tilde{W}_\alpha(\tau) = \int_{-\infty}^{+\infty} dv_z W_\alpha(v_z)\ \exp(ikv_z\tau), \qquad \Phi(\tau) = \int_{-\infty}^{+\infty} dv_z W_{ba}(v_z)\ \mathrm{sinc}(kv_z\tau)$$

Of course γ_α and γ_{ba} now include the velocity-changing departure rates as well as dephasing and quenching contributions. The collision kernels can now be calculated from the knowledge of the intermolecular potential. These functions are very strongly peaked around the initial velocity with a width of the order of 10^{-2} that of the Maxwell distribution. They will therefore play a major role in the line shape only when the line-width is of the order of 1% of the Doppler width. At very high resolution they give only a very broad and flat contribution and the width comes only from the transit time and from the total decay rate of the optical dipole. At intermediate resolution the collision kernels are responsible for an increase in pressure broadening. At low resolution they mostly act like delta-functions and compensate the departure decay rates coming from elastic collisions. At very high pressures the wings and the slightly asymmetric character of the kernels manifest themselves in the atomic case through a broad background, whereas in the molecular case, rotational relaxation dilutes this contribution from strong or multiple weak collisions over many levels. The saturated absorption line shape has thus a much richer content than what could be anticipated in the early days of saturation spectroscopy and some further interactions between theory and experiments are still necessary to get the full picture.

IV - RAMSEY INTERFERENCE FRINGES IN OPTICAL SPECTROSCOPY

A very elegant way out of the limitation imposed by transit-time broadening was proposed by N.F. RAMSEY in 1950 [13]. The proper way to extend this technique to sub-Doppler spectroscopy was discussed by Y.V. BAKLANOV and coll. very recently [14] and beautifully demonstrated by J. BERGQUIST and coll. [15] in the case of saturation resonances of CH_4 and Ne. The idea is to replace the large beam by two or more smaller field regions. To illustrate the principle of the method it is usual to describe the motion of the pseudo-spin but one gets an even simpler picture by considering the first-order perturbation term described by the diagram on figure 7.

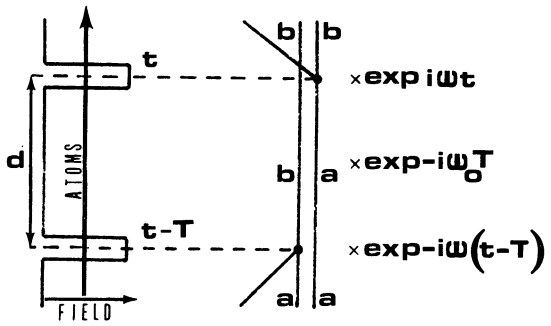

Figure 7

In the first field region a first interaction creates a dipole whose complex representation is proportional to the off-diagonal density matrix element ρ_{ba}. In the region free of field this dipole precesses at the Bohr frequency ω_o and therefore accumulates a phase angle $\omega_o T$ appearing in the corresponding propagator, where T is the time of flight across the distance d with velocity v. In the same time interval the field vector accumulates the phase angle ωT. The projection of the dipole on the second field is therefore multiplied by the factor exp i $(\omega-\omega_o)T$. If we add the complex conjugate diagram contribution we find that the power absorbed in the second zone is a broad function corresponding to the precise shape of each field region times cos $(\omega-\omega_o)d/v$ and that the line shape therefore exhibits fringes with an oscillation frequency proportional to the distance between the two regions of field. The integration over a velocity distribution will tend to destroy the side fringes and leave only the central one. Any fixed phase difference between the fields in both regions will appear in the cosine and displace the fringe system so that great care has to be taken to avoid this source of error in microwave spectroscopy.

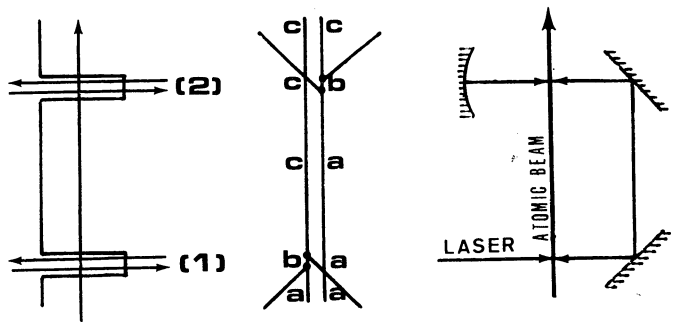

Figure 8

Figure 8 illustrates the extension of RAMSEY's idea to Doppler-free two-photon spectroscopy. This time we have at least two interactions in each field region, one with each of the two counter-propagating fields and it is the off-diagonal element ρ_{ca} which freely precesses between the two field regions. The phase factor that appears is exp $\left[i(\varphi_2^- + \varphi_2^+ - \varphi_1^- - \varphi_1^+)\right]$ where each φ comes frome one of the four fields. This total phase cancels out in a folded standing wave and this is precisely the geometry that was proposed by Y. BAKLANOV in [14]. The precise line shape with the relaxation and the Gaussian structure of the laser beams taken into account is derived in [16] where it is also shown that the beams need to be carefully matched to avoid shifts. In this case if $\Delta = 2\omega-\omega_{ca}$ is the detuning, β a real parameter depending upon the beam geometry (β is w^{-2} for beams having the same waist radius w) the fringes are proportionate to : exp $(-\Delta^2/4\beta v_r^2)$ cos $\left[\Delta\ (2\beta v_x d - \gamma_{ca})/2\beta v_r^2\right]$ where d is the distance between the beams in the x direction and $v_r^2 = v_x^2 + v_y^2$.

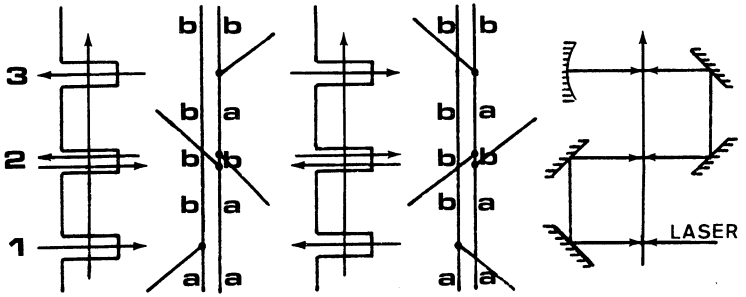

Figure 9

In saturation spectroscopy it is essential to add a third field region to the two others (figure 9). The reason for this third region lies in the fact that saturation spectroscopy is a two-step process : first the selection process of a velocity group, second the probing process of this selected group. Roughly speaking, to each of these two steps corresponds a response function and it is the convolution over v_z of these two functions that gives the final shape of the resonance. We must therefore repeat the RAMSEY operation twice : once to create a system of fringes on the population holes or peaks and a second time to probe this population change. If there were only two field zones, only one of these two steps would beneficiate from the narrowing, and the convolution with the second response function would average out the fringes. If we look at the time sequence on the fourth-order density matrix diagrams for one of the recoil peaks, we have a first interaction with one of the two waves in the first field zone giving a first-order dipole, which then freely precesses in the first dark zone and is turned into a population change with fringes in the v_z space. This population change interacts with the second wave in the central zone, gives a second dipole that precesses freely in the second dark zone to end up as energy absorbed for the last wave. Again there is a phase factor involving the fixed phases of the four fields : $\exp\left[i(\varphi_3^- - \varphi_2^- + \varphi_2^+ - \varphi_1^+) \right]$ which can be a source of shifts. Again the way out is the use of a folded standing wave. In this case we add the contribution of the second diagram of figure 9 where the first interaction is with the other choice in the first zone and the phases are such that the phase factor is complex conjugate of the first one. The asymmetric part of the two contributions versus frequency cancels out if the intensities of the two waves are identical (reflexion coefficent equal to one). This ideal situation of two waves of equal intensities was already required to cancel the curvature-induced shift [4,8] and we find here an analogous phenomenon. Some care has therefore to be taken to avoid these shifts. For small beam separations the cat's eye geometry proposed by J.C. BERGQUIST et al. [15] is even better than the simple folded standing wave since the total phase is identically zero. The line shape with relaxation and Gaussian beams is also derived in [16] . It is shown that the fringes disappear very quickly when the lengths of the dark zones differ from each other. In the special case of equal distances d and equal relaxation constants $\gamma_\alpha \equiv \gamma_{ba}$ it is found that the fringes are proportional to :

$$\exp\left[-(\omega-\omega_o)^2 w_o^2/v_r^2 \right] \cos\left[(\omega-\omega_o)\,(2v_x d/w_o^2 - \gamma_{ba})\, w_o^2/v_r^2 \right]$$

The strong-field numerical program [6] solving the coupled density matrix equations has also been found especially useful to study RAMSEY fringes.

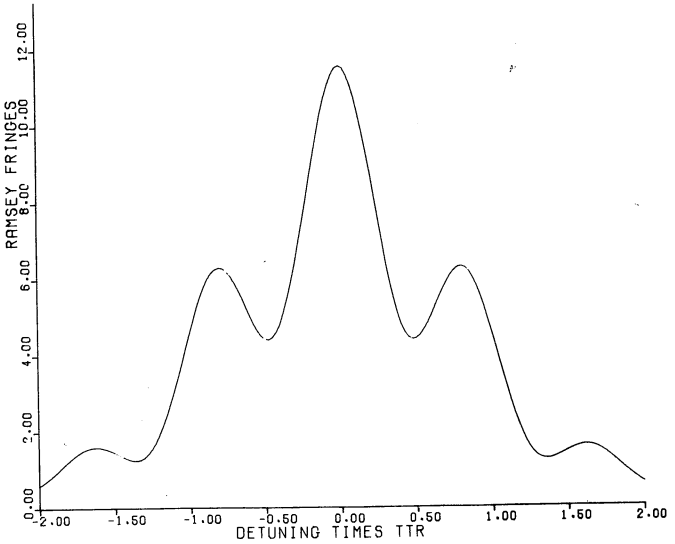

Figure 10

Figure 10 shows an example of application to three Gaussian beams separated by four times their beam waist redius w_o. The relaxation constants were all chosen equal to 0.1 and the two Rabi frequencies $\Omega^{\pm}$ equal to 0.01 in units of TTR = w_o/v_x. The same program gave asymmetric fringes for unequal beam intensities and a total phase different from zero. Some further confrontations between theory and experiments should bring us enough knowledge of these systematic effects to fully benefit from the increase of resolving power resulting from this beautiful technique.

Aknowledgment

I have shared the concern in the accuracy problem in high precision spectroscopy with Dr. John HALL for a number of years and many results of this paper are either a direct output or a consequence of our friendly collaboration.

REFERENCES

1. C.J. Bordé and J.L. Hall, in Laser Spectroscopy, edited by R.G. Brewer and A. Mooradian (Plenum, New York, 1974), pp. 125-142.
2. J.L. Hall and C.J. Bordé, Bull. Am. Phys. Soc. Series II, 19, 1196 (1974); J.L. Hall, C.J. Bordé and K. Uehara, Phys. Rev. Letters 37, 1339-1342

3. C.J. Bordé, C.R. Acad. Sc. Paris 283 B, 181-184 (1976)

4. C.J. Bordé, J.L. Hall, C.V. Kunasz and D.G. Hummer, Phys. Rev. A 14, 236-263 (1976)

5. J. Bordé and C.J. Bordé, C.R. Acad. Sc. Paris, to be published.

6. C.J. Bordé and J.L. Hall, Eighth International Quantum Electronics Conference, San Francisco (1974) ; C.J. Bordé, J.L. Hall and C.J. Kunasz, to be published

7. C.J. Bordé, C.R. Acad. Sc. Paris 282 B, 341-344 (1976)

8. J.L. Hall and C.J. Bordé, Appl. Phys. Letters 29, 788-790 (1976)

9. T.W. Hänsch, I.S. Shahin and A.L. Schawlow, Phys. Rev. Letters 27, 707 (1970)

10. S.N. Bagaev, E.V. Baklanov and V.P. Chebotaev, JETP Letters 16, 9-12 (1972)
T.W. Meyer, C.K. Rhodes and H.A. Haus, Phys. Rev. 12, 1993-2008 (1975)
L.S. Vasilenko, V.P. Kochanov and V.P. Chebotaev, Optics Comm. 20, 409-411 (1977)
A.T. Mattick, N.A. Kurnit and A. Javan, Chem. Phys. Letters 38, 176-180 (1976)

11. G. Camy, B. Decomps and C.J. Bordé, to be published

12. C.J. Bordé, S. Avrillier and M. Gorlicki, Journal de physique Lettres (July 1977)

13. N.F. Ramsey, Phys. Rev. 78, 695-699 (1950)

14. Y.V. Baklanov, B.Y. Dubetsky and V.P. Chebotaev, Applied Physics, 9, 171-173 (1976)
Y.V. Baklanov, V.P. Chebotaev and B.Y. Dubetsky, Appl. Phys. 11, 201 (1976)

15. J.C. Bergquist, S.A. Lee and J.L. Hall, Phys. Rev. Letters 38, 159-162 (1977)

16. C.J. Bordé, C.R. Acad. Sc. Paris 284B, 101-104 (1977)

OPTICAL RAMSEY FRINGES IN TWO-PHOTON SPECTROSCOPY

M.M. Salour

Department of Physics, Harvard University
Cambridge, MA 02138, USA

Interaction of atoms and molecules with intense monochromatic laser standing waves can give rise to very narrow Doppler-free two-photon resonances. This new high resolution spectroscopic method has recently been extensively applied to the study of several atomic and molecular optical transitions [1]. The discovery and accurate measurement of these narrow, frequency-stable resonance lines in the emission and absorption spectra of substances are significant because advances in this area will not only provide direct clues to the innermost processes of matter, but may also lead to novel applications in many areas of science.

The ultimate resolution achievable by the method of Doppler-free two-photon spectroscopy is limited in principle only by the natural linewidth of the excited state; in practice, however, the observed linewidth has thus far been limited by the laser. Thus in order to take full advantage of the elimination of the Doppler width, the spectral linewidth of the laser light must be as small as possible, which explains the motivation for using cw lasers. But, on the other hand, two-photon resonances require an appreciable intensity, and it is well known that pulsed dye lasers deliver higher powers and, furthermore, cover a broader spectral range. Recently, by using pulsed dye lasers pumped with an N_2 laser, it has been possible to observe two-photon resonances in several highly excited states of various atomic vapors which could not have been reached by cw excitation [2]. The resolution was limited by the spectral width $1/\tau$ of the pulse (τ: duration of each pulse), thus making it impossible to resolve many closely spaced two-photon resonance lines.

We have recently demonstrated [3] that, by exciting atoms with two time-delayed coherent laser pulses, one can obtain interference fringes in the profile of the Doppler-free two-photon resonances with a splitting $1/2T$ (T: delay between the two pulses) much smaller than the spectral width $1/\tau$ of the laser pulse (τ: duration of each pulse). This technique combined the advantages of pulsed dye lasers (power, spectral range) with the high resolution usually associated with a cw excitation, and could be considered as an extension, to two-photon Doppler-free resonances in the optical range, of the well-known Ramsey method of using two separated RF or microwave fields in atomic beam experiments [4].

Such an idea was first suggested in a slightly different context by BAKLANOV, CHEBOTAYEV AND DUBETSKII [5], who proposed using two spatially separated cw light standing waves. These authors considered two-photon